Ship observations over the southeast tropical Pacific Ocean for climate model evaluation

Simon de Szoeke[1,2], Paquita Zuidema[3], and Chris Fairall[1]

[1]*NOAA/ESRL Physical Sciences Division, Boulder, Colorado, USA*
[2]*CIRES, University of Colorado, Boulder, Colorado, USA*
[3]*Rosenstiel School of Marine and Atmospheric Science, University of Miami, Florida, USA*

Background

The mean climate, seasonal cycle, and interannual variability of the eastern tropical Pacific Ocean and atmosphere depend strongly on rich coupled atmosphere-ocean processes. Sea surface temperature (SST) depends on upwelling, offshore transport, and wind-evaporation-SST feedback, which are driven by wind along the shore of South America. Also among these processes, stratiform clouds cool the surface by shading solar radiation. Clouds are significant source of uncertainty to climate models, which have considerable errors in the eastern Pacific.

Because of its remoteness, few observations of the eastern tropical Pacific exist to quantify processes, improve parameterization, and assess and improve climate models. To address this deficiency, 6 NOAA research cruises were deployed in 2001 and 2003-2007 to 20˚S, 85˚W in the stratocumulus region offshore of Chile and Peru. Ships measured surface meteorology, turbulent and radiative fluxes, cloud thickness and optical properties, and aerosols, and profiled the atmosphere with rawinsondes.

Surface flux in GCMs: cloud errors and compensating errors

Ships outfitted with surface meteorology sensors capable of measuring surface fluxes traversed 75 to 85˚W along the 20˚S parallel in autumn of 2001 and 2003-2007. Fig. 2 shows ship fluxes along 20˚S (blue). Too much incoming solar radiation and too little outgoing longwave radiation are a sign of too little clouds in the models. Despite the strong solar radiation in models, excess longwave, sensible, and latent cooling result in *less* net surface warming than observed.

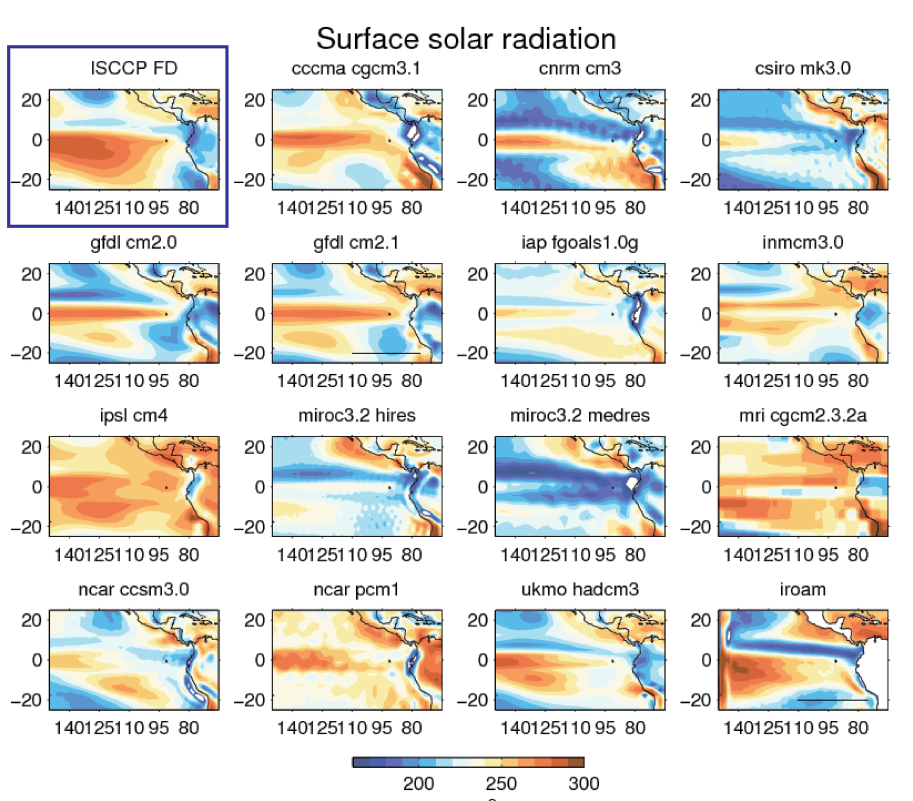

Figure 1. Models have a large variety of annual average surface solar radiation. Clouds are the largest contributor to the variety of modeled solar flux. ISCCP flux data are shown at the top left. Flux was measured by ships along 20˚S, 75-85˚W, and shown in Fig. 2.

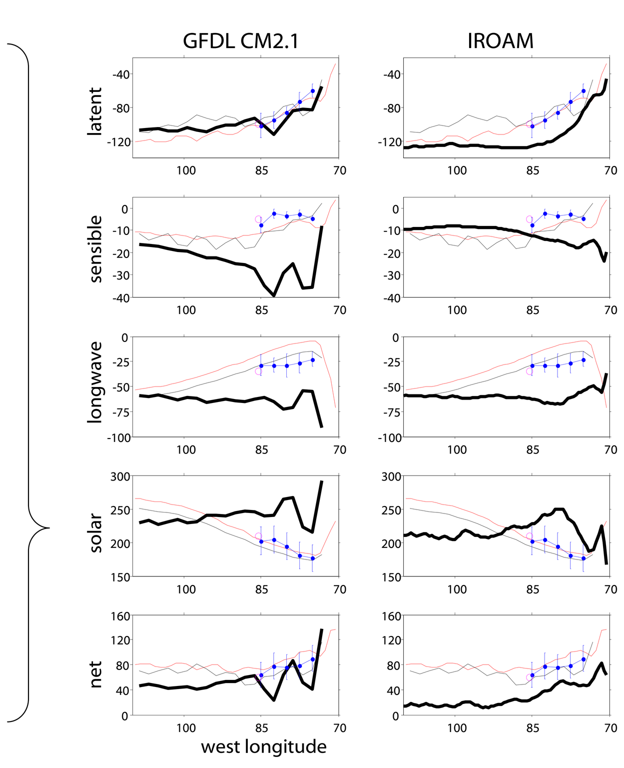

Figure 2. Flux analysis products for October (WHOI/ISCCP, red; CORE, black) agree with ship (blue) and buoy (magenta) observations along 20˚S, even where models (thick black) have most error. Model errors are consistent with too little cloud. Flux component errors nearly compensate in the net flux.

Coastal section in 2007

In 2007 the NOAA ship *Ron Brown* made an unique transect along the coast of South America, traveling within 300 km of shore. Fig. 7 shows the path of the ship with 6-hour red dashes. Blue vectors show the surface wind, which was nearly parallel to the coast. SST (red), surface air temperature (blue), humidity (green), and wind speed (black dashed) along the track are displayed as a function of latitude to the left. There are two distinct regimes: warm equatorial water greater than 20˚C north of 2˚S and cool southern-hemisphere water (~18˚C). The sea-air temperature difference was more than 2˚C near the equator and less than 1˚C in the south, resulting in a very large gradient in the evaporation E, and a large relative change in the sensible heat flux H (black lines). Radiative fluxes are shown in red.

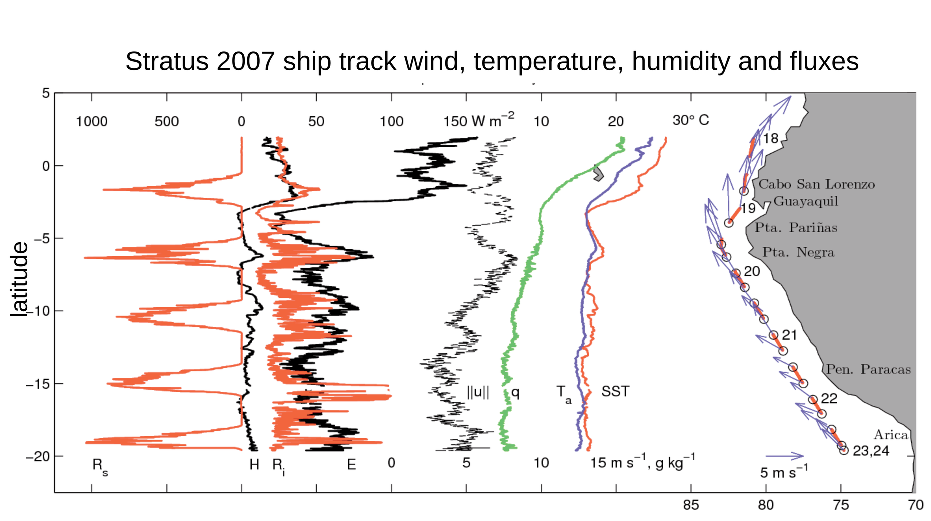

Figure 7. Track of the ship, wind vectors, SST (red), surface air temperature T_a (blue), specific humidity q (green), and wind speed ||u||. Radiative fluxes R_s and R_l at left are plotted in red, turbulent fluxes H and E are plotted in black. Numbers along the track indicate the date of October. Circles show the locations of soundings shown in Fig. 8.

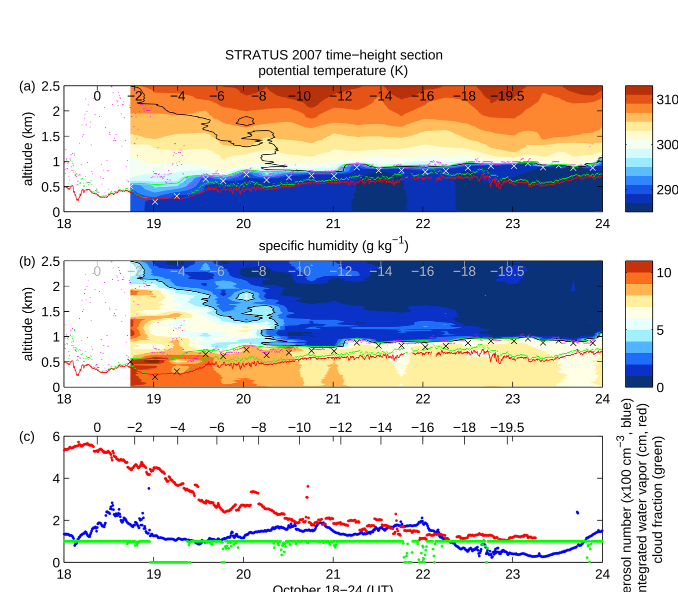

Figure 8. Time-height series of sounding (a) potential temperature and (b) specific humidity along the coastal section. Panel (c) shows aerosol concentration (blue, cm^{-3}), water vapor path (red, cm), and cloud fraction (green).

Soundings over the warmer water (before October 20, Fig. 8) reveal an indistinct boundary layer, with moisture rising above 1 km, and maximum scattering of the 915 GHz radar at a variety of levels rather than at a particular trade inversion. Here the free troposphere was frequently penetrated by moist convection. Cloud bases (green) and LCLs (red) in panels (8a) and (8b) coincide over the warm water, and integrated water vapor path is larger here. Subsequent to 20 October, a typical marine trade-wind inversion-capped boundary layer is evident, with a relatively dry free troposphere. On 22-23 October the cloud base descends ~200 m and coincident aerosol concentrations dip from 200 to less than 50 particles per cm^3. The visible satellite image in Fig. 9 shows that the ship encountered a rift or a pocket of open cells (POC) in the clouds

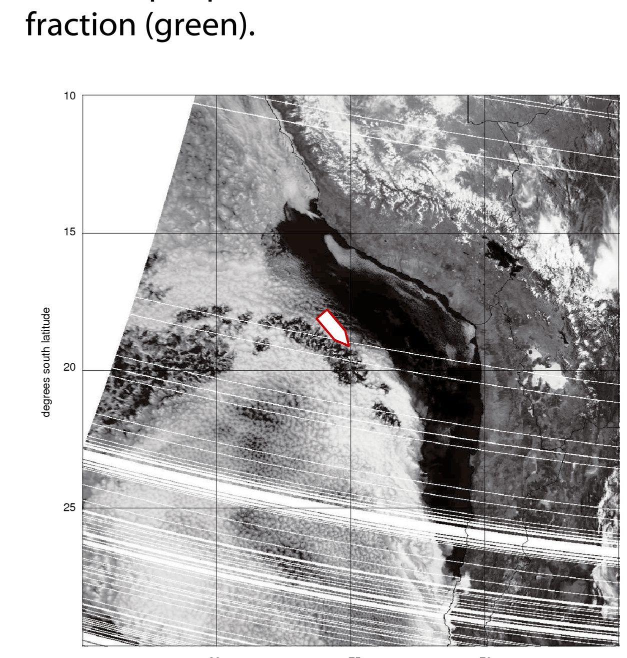

Figure 9. Visible radiance from the NOAA-17 polar-orbiting satellite on October 22 at 14:25 UT. At the time of the image, the ship was at the position marked (18.6˚S, 75.4˚W) between the clear boundary layer neighboring the coast and the rift or POC to the southwest.

Cloud observations from ships

Digital global positioning system (GPS) rawinsondes were released the ships, profiling the temperature, humidity, and winds in the atmosphere. Fig. 3 shows the potential temperature (left) and specific humidity (right panels) with color shading in the lower 2.5 km of the atmosphere along 20˚S, 75-85˚W for cruises in 2001, 2003, 2004, 2006, and 2007. The potential temperature and humidity both show a well-mixed marine boundary layer strongly capped by a trade inversion, beneath the stratified free troposphere. Where soundings are available, the 296 K potential temperature (green) and 4 g kg^{-1} specific humidity (black) contours describe the height of the trade inversion well. The crosses in Fig. 3 show the height of the temperature minimum at the inversion base.

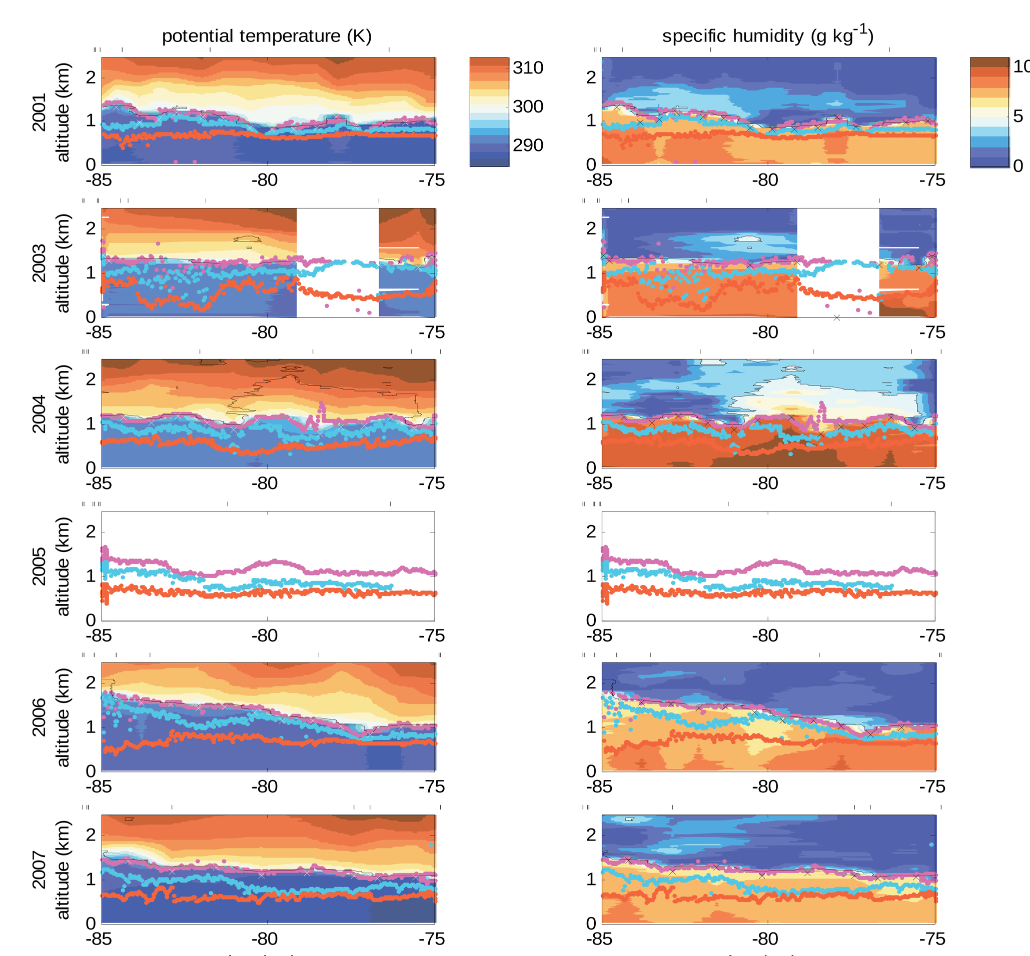

Figure 3. Potential temperature and specific humidity soundings. The 296 K (green) and 4 g kg^{-1} (black) contours mark the inversion. Crosses mark the inversion base. Magenta dots show the height of the inversion from a radar profiler. Cyan dots mark the stratocumulus cloud base measured by a lidar ceilometer. Red dots mark the lifting condensation level (LCL) of a surface parcel.

Cloud heights are measured by radar and lidar instruments on the ship. Pulses from a 915 MHz wind profiler are scattered by refractive index changes at the inversion. Magenta dots show the inversion height in Fig. 3. Cloud top height is believed to be below the inversion, near the inversion base. Cloud base is located by a lidar ceilometer. The inversion rises noticeably toward the west in 2001, 2005, 2006, and 2007, as expected of a cold-advection boundary layer traveling westward over progressively warmer water.

In Fig. 4 the cloud top and base height and the LCL of all 6 cruises are averaged in 2.5˚ longitude bins. The inversion and cloud base rise to the west, while the cloud thickness and LCL remain constant. The separation between the surface parcel LCL and the stratocumulus cloud base indicates entrainment of free-troposphere air drying the boundary layer. Figure 5 shows integrated liquid and vapor path from a 2-channel 20.6 and 31.65 GHz passive microwave radiometer, averaged over all cruises along 20˚S. While water vapor path is constant from 75-85˚W, the liquid water path increases to the west.

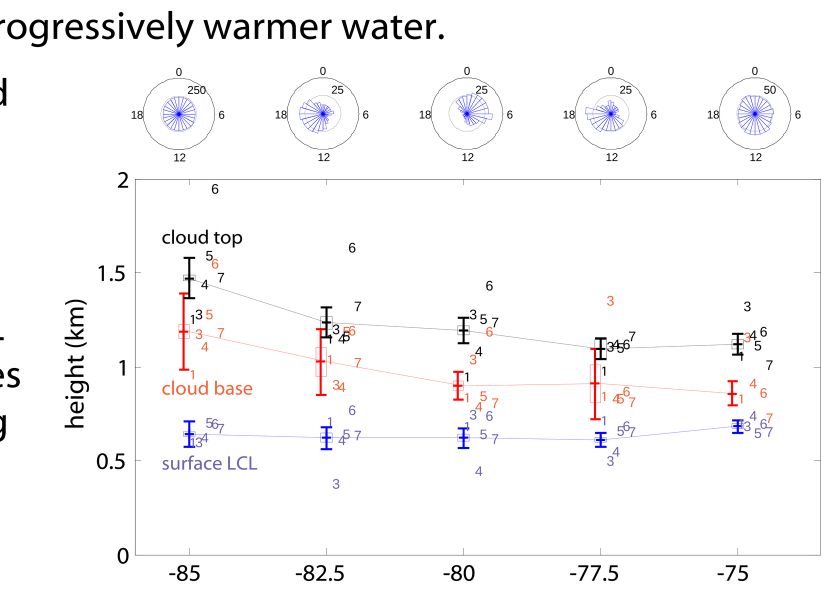

Figure 4. Cloud top and base heights, and surface LCL. Averages for each cruise are plotted as the last digit of the cruise year.

The roses at the top of Fig. 4 are 24-hour clock histograms showing the number of samples at each longitude as a function of local time. There are many samples around the clock at 75 and 85˚W because the ship was stationed there, but there are diurnal sampling biases between where the ship was underway. The diurnal cycle of cloud base and height, and column-integrated liquid and vapor are shown in Fig. 6. From midnight to 8 hours cloud thickness exceeds 300 m and the cloud rises 50 m. From 8-17 hours the top sinks 150 m; at 12 the thickness is minimal at 75 m. From sunset to midnight, the cloud base is constant and the top grows 100 m. Liquid water path is minimal in the afternoon at 50 g m^{-2}, and maximal before sunrise at 145 g m^{-2}. Water vapor path and LCL are relatively constant at 20 mm and 650 m, respectively.

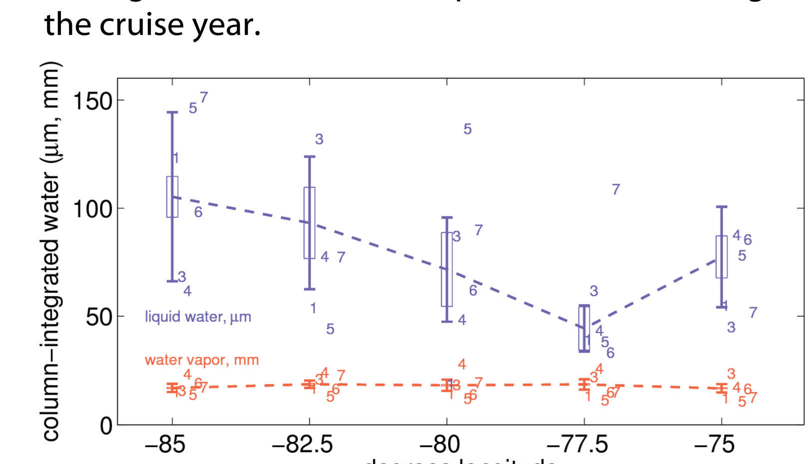

Figure 5. Liquid water path (g m^{-2} or 10^{-3} mm) and water vapor path (mm) along 20˚S.

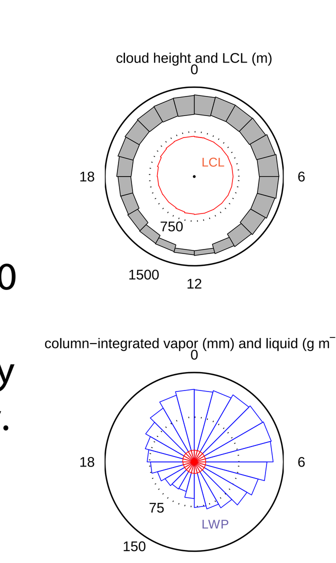

Figure 6. 24-hour rose plots of the diurnal cycle of clouds composited on local time along 20˚S, 75-85˚W. *Top*: cloud base and top height (m) composite over the diurnal cycle, with cloud vertical extent shaded gray. LCL is shown in red. *Bottom*: Liquid water path (g m^{-2}) and water vapor path (mm) diurnal cycle composite.

Summary

Observations of clouds, surface meteorology, and fluxes are available from 6 years of Stratus cruises to the southeastern tropical Pacific. These data provide context for the upcoming VAMOS Ocean Cloud Atmosphere Land Study (VOCALS) regional experiment planned for October 2008, and provide ground truth provide ground-truth for verifying and improving climate models in a region where they have large errors. The observations from all cruises have been averaged to a consistent format, and are provided for download on the web:
http://www.esrl.noaa.gov/psd/people/Simon.deSzoeke/synthesis.html
or by emailing Simon.deSzoeke@noaa.gov.

References

Fairall, C. W., T. Uttal, D. Hazen, J. Hare, M. F. Cronin, N. Bond, D. E. Veron, 2008: Observations of cloud, radiation, and surface forcing in the equatorial eastern Pacific. *J. Climate*, **21**, 4, 655-673.

de Szoeke, S. P. and S.-P. Xie, 2008: The tropical eastern Pacific seasonal cycle: Assessment of errors and mechanisms in IPCC AR4 coupled ocean-atmosphere general circulation models. *J. Climate*, **21**, 11, 2573–2590.

de Szoeke, S. P., C. W. Fairall, and Sergio Pezoa, 2008: Ship observations coasting South America in the tropical Pacific Ocean. *J. Climate*, submitted.

Zuidema, P., E. R. Westwater, C. Fairall, and D. Hazen, 2005: Ship-based liquid water path estimates in marine stratocumulus. *J. Geophys. Res.* **110**, D20206, doi: 10.1029/2005DJ005833.